Spectroscopy and Reactivity of the Type 1 Copper Site in Fet3p from *Saccharomyces cerevisiae*: Correlation of Structure with Reactivity in the Multicopper Oxidases

Timothy E. Machonkin,[†] Liliana Quintanar,[†] Amy E. Palmer,[†] Richard Hassett,[‡] Scott Severance,[‡] Daniel J. Kosman,[‡] and Edward I. Solomon*,[†]

Contribution from the Department of Chemistry, Stanford University, Stanford, California 94305, and Department of Biochemistry, School of Medicine and Biomedical Sciences, State University of New York, Buffalo, New York 14214

Received November 15, 2000. Revised Manuscript Received March 28, 2001

Abstract: Fet3p is a multicopper oxidase recently isolated from the yeast, *Saccharomyces cerevisiae*. Fet3p is functionally homologous to ceruloplasmin (Cp) in that both are ferroxidases. However, by sequence homology Fet3p is more similar to fungal laccase, and both contain a type 1 Cu site that lacks the axial methionine ligand present in the functional type 1 sites of Cp. To determine the contribution of the electronic structure of the type 1 Cu site of Fet3p to the ferroxidase mechanism, we have examined the absorption, circular dichroism, magnetic circular dichroism, electron paramagnetic resonance, and resonance Raman spectra of wild-type Fet3p and type 1 and type 2 Cu-depleted mutants. The spectroscopic features of the type 1 Cu site of Fet3p are nearly identical to those of fungal laccase, indicating a very similar three-coordinate geometry. We have also examined the reactivity of the type 1 Cu site by means of redox titrations and stopped-flow kinetics. From poised potential redox titrations, the E° of the type 1 Cu site is 427 mV, which is low for a three-coordinate type 1 Cu site. The kinetics of reduction of the type 1 Cu sites of four different multicopper oxidases with two different substrates were compared. The type 1 site of a plant laccase (*Rhus vernicifera*) is reduced moderately slowly by both Fe(II) and a bulky organic substrate, 1,4-hydroquinone (with 6 equiv of substrate, $k_{obs} = 0.029$ and 0.013 s^{-1}, respectively). On the other hand, the type 1 site of a fungal laccase (*Coprinus cinereus*) is reduced very rapidly by both substrates ($k_{obs} > 23$ s^{-1}). In contrast, both Fet3p and Cp are rapidly reduced by Fe(II) ($k_{obs} > 23$ s^{-1}), but only very slowly by 1,4-hydroquinone (10- and 100-fold more slowly than plant laccase, respectively). Semiclassical theory is used to analyze the origin of these differences in reactivity in terms of type 1 Cu site accessibility to specific substrates.

Introduction

The multicopper oxidases are an important class of enzymes found in bacteria, fungi, plants, and animals. These enzymes couple the four-electron reduction of O_2 to water with four sequential one-electron oxidations of substrate. This redox reaction depends on the presence of four Cu atoms that are classified into three types of Cu sites, i.e., type 1 (T1), type 2 (T2), and type 3 (T3).[1] The best studied members of this enzyme class are *Rhus vernicifera* (Japanese lacquer tree) laccase (Lc), fungal Lc, ascorbate oxidase (AO), and human ceruloplasmin (hCp). Extensive spectroscopic and kinetic studies have been done on *R. vernicifera* Lc.[1] Spectroscopic[2] and steady-state kinetic[3] studies have been done on the fungal Lc's, and a crystal structure has been reported for a T2 Cu-depleted form of *Coprinus cinereus* Lc.[4] AO, which resembles a dimer of Lc, has been crystallographically characterized in the oxidized[5] and reduced[6] states. hCp is the most complex of the multicopper oxidases: it contains two additional T1 copper atoms. Crystal structures exist for the resting oxidized[7] and metal-,[8] organic substrate-, and N_3^--bound forms[9] of hCp. We have shown that one of the T1 Cu sites in hCp (T1PR) remains permanently reduced.[10] Recently, the complex kinetics of intramolecular electron transfer (ET) in hCp have been probed.[11]

T1 or blue Cu sites are characterized by an intense Cys S-to-Cu(II) charge-transfer (CT) band at ∼600 nm. The electron paramagnetic resonance (EPR) spectrum exhibits $g_{||} > g_\perp > 2.00$, indicative of a $d_{x^2-y^2}$ ground state, and narrow parallel hyperfine splitting [$A_{||} = (43-95) \times 10^{-4}$ cm^{-1}], originating from the highly covalent Cu $d_{x^2-y^2}$−Cys S π bond.[12,13] The

* To whom correspondence should be addressed. Phone: (650) 723-4694. E-mail: edward.solomon@stanford.edu.
† Stanford University.
‡ State University of New York.

(1) Solomon, E. I.; Sundaram, U. M.; Machonkin, T. E. *Chem. Rev.* **1996**, *96*, 2563−2605.
(2) Palmer, A. E.; Randall, D. W.; Xu, F.; Solomon, E. I. *J. Am. Chem. Soc.* **1999**, *121*, 7138−7149.
(3) Xu, F. *Biochemistry* **1996**, *35*, 7608−7614.
(4) Ducros, V.; Brzozowski, A. M.; Wilson, K. S.; Brown, S. H.; Østergaard, P.; Schneider, P.; Yaver, D. S.; Pedersen, A. H.; Davis, G. J. *Nat. Struct. Biol.* **1998**, *5*, 310−316.
(5) Messerschmidt, A.; Ladenstein, R.; Huber, R.; Bolognesi, M.; Avigliano, L.; Petruzzelli, R.; Rossi, A.; Finazzi-Agro, A. *J. Mol. Biol.* **1992**, *224*, 179−205.
(6) Messerschmidt, A.; Luecke, H.; Huber, R. *J. Mol. Biol.* **1993**, *230*, 997−1014.
(7) Zaitseva, I.; Zaitsev, V.; Card, G.; Moshov, K.; Bax, B.; Ralph, A.; Lindley, P. *J. Biol. Inorg. Chem.* **1996**, *1*, 15−23.
(8) Lindley, P. F.; Card, G.; Zaitseva, I.; Zaitsev, V.; Reinhammar, B.; Selin-Lindgren, E.; Yoshida, K. *J. Biol. Inorg. Chem.* **1997**, *2*, 454−463.
(9) Zaitsev, V. N.; Zaitseva, I.; Papiz, M.; Lindley, P. F. *J. Biol. Inorg. Chem.* **1999**, *4*, 579−587.
(10) Machonkin, T. E.; Zhang, H. H.; Hedman, B.; Hodgson, K. O.; Solomon, E. I. *Biochemistry* **1998**, *37*, 9570−9578.
(11) Machonkin, T. E.; Solomon, E. I. *J. Am. Chem. Soc.* **2000**, *122*, 12547−12560.

10.1021/ja003975s CCC: $20.00
Published on Web 05/15/2001

circular dichroism (CD) and magnetic circular dichroism (MCD) spectra are dominated by intense ligand field (LF) transitions, which are a sensitive probe of the geometric and electronic structure of the Cu site.[12−15] The T1 Cu site found in the multicopper oxidases functions in long-range ET, shuttling electrons from substrate to the other Cu sites. In fungal Lc, the T1 Cu lies at the bottom of a shallow bowl and is directly solvent-accessible, while in AO and hCp there are distinct substrate-binding pockets adjacent to the T1 Cu.

The T2 or normal Cu site is characterized by the lack of strong absorption bands and has a $d_{x^2-y^2}$ ground state with $g_{||} > g_{\perp} > 2.00$ and large parallel hyperfine splitting [$A_{||} = (158-201) \times 10^{-4}$ cm^{-1}] in the EPR spectrum. The T3 or coupled binuclear Cu site is characterized by an intense CT band at ∼330 nm, originating from a bridging hydroxide. It lacks an EPR signal due to strong isotropic exchange coupling mediated by the hydroxide bridge. Together, the T2 and T3 Cu sites form a trinuclear Cu cluster that is the site for O_2 reduction.[5,16−18] The trinuclear cluster is coupled to the T1 Cu site via a 13 -Å cysteine−histidine ET pathway. By substitution of the T1 Cu site with Hg(II) in *R. vernicifera* Lc (T1HgLc), the electronic transitions of the T2 and T3 Cu sites, normally obscured by the intense T1 Cu bands, have been examined.[19,20] The T2 Cu has a number of weak LF bands in the MCD spectrum, but no bands evident in the CD spectrum, due to the approximately planar geometry of this site.[19] The T3 Cu does not exhibit MCD bands, due to the antiferromagnetic coupling of the Cu(II) ions, but does exhibit a number of weak LF bands in the CD spectrum, due to the low symmetry around each Cu(II).[19,20]

Cp was originally the only multicopper oxidase known to possess ferroxidase activity.[21−26] However, the *FET3* gene in the high-affinity Fe-uptake system of *Saccharomyces cerevisiae* encodes a membrane-bound multicopper oxidase with ferroxidase activity, Fet3p.[27,28] Fet3p shows a high degree of sequence homology to the other multicopper oxidases, particularly in the conserved Cu-binding regions.[28] However, this sequence analysis indicates that the T1 Cu site of Fet3p lacks the typical Met axial ligand common to many type 1 copper sites in other blue copper proteins. This position in the sequence is occupied by Leu. This lack of an axial ligand is also found in the fungal Lc's[1,4] and in one of the three type 1 Cu sites (the T1PR site) of hCp.[7,29,30] The membrane-spanning C-terminal domain of Fet3p has been removed by mutagenesis to yield a soluble enzyme, which has been characterized by absorption, EPR, and steady-state kinetics.[31−33] The absorption and EPR spectra of Fet3p show the typical spectroscopic signatures of T1, T2, and T3 Cu sites.[32,33] From the steady-state kinetics of Fet3p, the K_m values for Fe(II) and O_2 are 4.8 and 1.3 μM, respectively, and the k_{cat} values for Fe(II) and O_2 are 9.5 and 2.3 min^{-1}, respectively.[31,33] For comparison, in hCp the k_{cat} for Fe(II) is 138 or 550 min^{-1} (depending upon the method of analysis), while the K_m is of the same order of magnitude as in Fet3p.[25,26]

Several other gene components constitute the high-affinity Fe uptake system of *S. cerevisiae* (for reviews, see refs 34 and 35), most importantly *FTR1*, which transports Fe across the plasma membrane after it is oxidized by Fet3p.[36] The activities of Fet3p and Ftr1p are closely connected, and they likely form an enzyme complex on the cell surface.[36]

Very recently, three different Cu site mutants of Fet3p have been generated and characterized: a T2-depleted (T2D) mutant in which the T2 Cu ligand His81 is mutated to Gln, a T1-depleted (T1D) mutant in which the T1 Cu ligand Cys484 is mutated to Ser, and a T1- and T2-depleted double mutant (T1D/T2D).[37] In each of these mutants, the absorption and EPR spectra of the remaining Cu sites were essentially unaltered from that of wild-type (wt) enzyme.[38] This showed that selective removal of the T1 and/or T2 Cu sites could be accomplished by mutagenesis without altering the remaining Cu sites, greatly facilitating the detailed spectroscopic study of the Cu sites of Fet3p. The initial report focused on examination of the trinuclear cluster by extended X-ray absorption fine structure (EXAFS).[37] The EXAFS data of the T1D mutant were very similar to those of T1HgLc.[18,39] This, together with EXAFS on the T1D/T2D mutant, showed that the first coordination sphere of the trinuclear cluster of Fet3p is essentially the same as that of AO, as determined by X-ray crystallography.

Although Fet3p is functionally homologous to hCp, it has the unusual T1 Cu site with no axial Met ligand seen only in the fungal Lc's and in the redox-inactive T1PR site of hCp. The crystal structure of *C. cinereus* Lc showed that this site is three-coordinate.[4] Detailed spectroscopic and electronic structure studies of the T1 Cu sites of several fungal Lc's have been reported.[2] The lack of an axial Met ligand in the T1 Cu site in

(12) Gewirth, A. A.; Solomon, E. I. *J. Am. Chem. Soc.* **1988**, *110*, 3811−3819.
(13) Solomon, E. I.; Penfield, K. W.; Gewirth, A. A.; Lowery, M. D.; Shadle, S. E.; Guckert, J. A.; LaCroix, L. B. *Inorg. Chim. Acta* **1996**, *243*, 67−78.
(14) LaCroix, L. B.; Shadle, S. E.; Wang, Y.; Averill, B. A.; Hedman, B.; Hodgson, K. O.; Solomon, E. I. *J. Am. Chem. Soc.* **1996**, *118*, 7775−7768.
(15) LaCroix, L. B.; Randall, D. W.; Nersissian, A. M.; Hoitink, C. W. G.; Canters, G. W.; Valentine, J. S.; Solomon, E. I. *J. Am. Chem. Soc.* **1998**, *120*, 9621−9631.
(16) Allendorf, M. D.; Spira, D. J.; Solomon, E. I. *Proc. Natl. Acad. Sci. U.S.A.* **1985**, *82*, 3063.
(17) Spira-Solomon, D. J.; Allendorf, M. D.; Solomon, E. I. *J. Am. Chem. Soc.* **1986**, *108*, 5318.
(18) Cole, J. L.; Tan, G. O.; Yang, E. K.; Hodgson, K. O.; Solomon, E. I. *J. Am. Chem. Soc.* **1990**, *112*, 2243−2249.
(19) Cole, J. L.; Clark, P. A.; Solomon, E. I. *J. Am. Chem. Soc.* **1990**, *112*, 9534−9548.
(20) Sundaram, U. M.; Zhang, H. H.; Hedman, B.; Hodgson, K. O.; Solomon, E. I. *J. Am. Chem. Soc.* **1997**, *119*, 12525−12540.
(21) Lahey, M. E.; Gubler, C. J.; Chase, M. S.; Cartwright, G. E.; Wintrobe, M. M. *Blood* **1952**, *7*, 1053−1074.
(22) Osaki, S.; Johnson, D. A. *J. Biol. Chem.* **1969**, *244*, 5757−5765.
(23) Ragan, H. A.; Nacht, S.; Lee, G. R.; Bishop, C. R.; Cartwright, G. E. *Am. J. Phys.* **1969**, *217*, 1320−1323.
(24) Roeser, H. P.; Lee, G. R.; Cartwright, G. E. *J. Clin. Invest.* **1970**, *49*, 2408−2417.
(25) Osaki, S. *J. Biol. Chem.* **1966**, *241*, 5053−5059.
(26) Huber, C. T.; Frieden, E. *J. Biol. Chem.* **1970**, *245*, 3973−3978.
(27) Askwith, C.; Eide, D.; Van Ho, A.; Bernard, P. S.; Li, L.; Davis-Kaplan, S.; Sipe, D. M.; Kaplan, J. *Cell* **1994**, *76*, 403−410.
(28) de Silva, D.; Askwith, C. C.; Eide, D.; Kaplan, J. *J. Biol. Chem.* **1995**, *270*, 1098−1101.
(29) Yang, F.; Naylor, S. L.; Lum, J. B.; Cutshaw, S.; McCombs, J. L.; Naberhaus, K. H.; McGill, J. R.; Adrian, G. S.; Moore, C. M.; Barnett, D. R.; Bowman, B. H. *Proc. Natl. Acad. Sci. U.S.A.* **1986**, *83*, 3257−3261.
(30) Koschinsky, M. L.; Funk, W. D.; Oost, B. A. v.; MacGillivray, R. T. A. *Proc. Natl. Acad. Sci. U.S.A.* **1986**, *83*, 5086−5090.
(31) de Silva, D.; Davis-Kaplan, S.; Fergestad, J.; Kaplan, J. *J. Biol. Chem.* **1997**, *272*, 14208−14213.
(32) Kosman, D. J.; Hassett, R.; Yuan, D. S.; McCracken, J. *J. Am. Chem. Soc.* **1998**, *120*, 4037−4038.
(33) Hassett, D. J.; Yuan, D. S.; Kosman, D. J. *J. Biol. Chem.* **1998**, *273*, 23274−23282.
(34) Askwith, C.; Kaplan, J. *Trends Biochem. Sci.* **1998**, *23*, 135−138.
(35) Radisky, D.; Kaplan, J. *J. Biol. Chem.* **1999**, *274*, 4481−4484.
(36) Stearman, R.; Yuan, D. S.; Yamaguchi-Iwai, Y.; Klausner, R. D.; Dancis, A. *Science* **1996**, *271*, 1552−1557.
(37) Blackburn, N. J.; Ralle, M.; Hassett, R.; Kosman, D. J. *Biochemistry* **2000**, *39*, 2316−2324.
(38) Although all of the forms of Fet3 studied are mutants in the sense that the C-terminal transmembrane domain has been removed by mutagenesis, we use the term "wild-type" to refer to enzyme with no modifications of the amino acids coordinated to the Cu sites.
(39) Shin, W.; Sundaram, U. M.; Cole, J. L.; Zhang, H. H.; Hedman, B.; Hodgson, K.; Solomon, E. I. *J. Am. Chem. Soc.* **1996**, *118*, 3202−3215.

the fungal Lc's results in an increase in the ligand field strength and in the $Cu-S_{Cys}$ covalency relative to the classical four-coordinate blue Cu site in plastocyanin (Pc), which results in a stronger $Cu-S_{Cys}$ bond. This study also confirmed that the lack of an axial Met ligand results in a 100 mV increase in the reduction potential of the site, consistent with mutagenesis studies done on a typical four-coordinate blue Cu protein,[40] and this indicates that the axial Met ligand is an important factor contributing to the T1 Cu site redox potential.

Given that Fet3p shares the same unusual T1 Cu ligand set as fungal Lc, yet it is functionally similar to Cp, the focus of the present study is to explore the spectroscopy of this site in detail in order to compare it to the well-defined three-coordinate T1 Cu site of fungal Lc. This helps to define the role of the geometric and electronic structure of this site in the ferroxidase mechanism. Since the T2D and T1D mutants allow one to isolate the spectroscopic features of specific Cu sites, we have examined the absorption, CD, MCD, EPR, and resonance Raman (RR) spectra of these mutants as well as the wild-type enzyme. Some difficulties were experienced with the T2D mutant, but the spectral features of the T1 Cu could be obtained by comparison of the wild-type and T1D forms. We have also determined the reduction potential of this site for comparison to the other multicopper oxidases. Finally, we have explored the reactivity of the T1 Cu site with Fe(II) and an outer-sphere substrate (1,4-hydroquinone) by stopped-flow kinetics in order to probe substrate specificity relative to *R. vernicifera* Lc and *C. cinereus* Lc, which have no substrate binding pocket, and hCp, which shows a high selectivity for Fe(II).

Experimental Section

Water was purified to a resistivity of 15.5−17 MΩ cm^{-1} using a Barnstead Nanopure deionization system. All chemicals were reagent grade and used without further purification. Expression, isolation, purification, and characterization of wt, T2D, and T1D Fet3p were done as previously described.[33,37] Fresh human plasma was obtained from the Stanford Blood Center, and hCp was purified from it by a rapid one-step method,[41] modified as previously described.[10] hCp was oxidized by H_2O_2 and then assayed for purity, protein concentration, and Cu content as previously described.[10] *R. vernicifera* Lc was purified from the acetone powder (Saito and Co., Osaka, Japan) using the standard literature procedures.[42,43] *Coprinus cinereus* laccase was obtained from the University of York. All samples were used immediately or kept frozen at −80 °C until use.

Absorption spectra were recorded at room temperature (25 °C) on a Hewlett-Packard HP8452A diode array UV−visible absorption spectrophotometer. EPR spectra were obtained with a Bruker ER 220-D-SRC spectrometer. Sample temperatures were maintained at 77 K using a liquid N_2 finger dewar. EPR spectra were spin quantitated with a 1.0 mM aqueous copper standard run in the same tube as the sample where possible.[44] CD spectra at 4 °C were obtained in the UV−visible region with a Jasco J-500-C spectropolarimeter and an S-20 photomultiplier tube, and in the near-IR region with a Jasco J-200-D spectropolarimeter and a liquid N_2-cooled InSb detector. For MCD, the magnetic field was supplied by either an Oxford SM4 or SM4000 7 T superconducting magnetooptical dewar. The MCD sample cells consisted of two quartz disks with a 3-mm rubber spacer. The data were corrected for zero-field baseline effects induced by cracks in the glass by subtracting the corresponding 0 T scan. RR spectra were collected with a Princeton Instruments ST-135 back-illuminated CCD detector on a Spex 1877 CP triple monochromator with 1200, 1800, and 2400 grooves/mm holographic spectrograph gratings. A Coherent Kr^+ ion laser provided excitation at 647.1 nm. A polarization scrambler was used between the sample and the monochromator. The Raman scattering energy was calibrated with proprionitrile. Raman shifts are accurate to within <2 cm^{-1}. Samples were loaded into 3 mm o.d. quartz tubes and spun by an air-driven NMR tube spinner. RR sample temperatures were maintained at <200 K with a N_2 flow system. Stopped-flow absorption kinetics were obtained with an Applied Photophysics RX2000 with a path length of 1 cm. The tubing system was made anaerobic by washing with a dithionite solution followed by repeated washings with degassed water and/or buffer. O_2 was excluded by passage of a stream of N_2 through the system. The absorption data were collected on the Hewlett-Packard HP8452A diode array spectrophotometer. The temperature was 25 °C.

Reduction potentials of the T1 Cu were obtained by the poised potential method. To a 200 μL sample of ∼0.1 mM degassed wt FET3p in a 1 cm path length anaerobic cuvette with a Teflon stopcock was added degassed $K_3[Fe(CN)_6]$ to yield a final concentration of ∼5 mM. Aliquots of degassed $K_4[Fe(CN)_6]$ were added, and absorption spectra were taken at room temperature over time until equilibrium was achieved for each titration point.

For all of the spectroscopic measurements except RR, Fet3p was in deuterated 50 mM MES buffer with a pD of 6.5 and with 50 vol % of deuterated glycerol (in order to form an optical-quality glass upon freezing) and a protein concentration of ∼0.5 mM. For the RR spectra, the conditions were the same except no glycerol was added. The presence or absence of glycerol had no effect on the Cu sites, as assessed by EPR. For Fet3p, the poised potential and stopped-flow kinetic measurements were performed in both nondeuterated pH 6.5 MES buffer and nondeuterated pH 7.0 potassium phosphate buffer without glycerol. The kinetic measurements on *R. vernicifera* Lc and hCp were done in pH 7.0 phosphate buffer. For all the kinetic measurements, the protein concentration was 35 μM.

EPR simulations were performed with the program Qpowa6 available from L. Belford at the University of Illinois (Illinois ESR Research Center, NIH Division of Research Resources Grant No. RR01811).[45,46] Calculations of intramolecular ET pathways were performed with the Pathways program based upon the work primarily of Beratan and Onuchic[47−56] and obtained from Jeffrey Regan. The crystal structures of hCp and *C. cinereus* Lc were obtained from the Protein Data Bank (1KCW and 1A65, respectively). Protons were added with Insight II, and lone pairs were added with Pathways. Solvent accessibility and protein structure visualization were performed with Rasmol.

Results and Analysis

1. Spectroscopy. 1.1. Absorption, CD, MCD, EPR, and RR Spectra of Wild-Type Fet3p and Cu Site Mutants. The absorption, CD, and MCD spectra of wt and the T2D and T1D mutants of Fet3p were used to selectively probe the electronic

(40) Pascher, T.; Karlsson, B. G.; Nordling, M.; Malmström, B. G.; Vänngård, T. *Eur. J. Biochem.* **1993**, *212*, 289−296.
(41) Calabrese, L.; Mateescu, M. A.; Carbonaro, M.; Mondovi, B. *Biochem. Int.* **1988**, *16*, 199−208.
(42) Reinhammar, B. *Biochim. Biophys. Acta* **1970**, *205*, 35.
(43) Reinhammar, B. R. M. *Biochim. Biophys. Acta* **1972**, *275*, 245−259.
(44) Carithers, R. P.; Palmer, G. *J. Biol. Chem.* **1981**, *256*, 7967−7976.
(45) Nilges, M. J., Ph.D. Thesis; University of Illinois: Urbana, IL, 1979.
(46) Belford, R. L., Nilges, M. J., Eds. *Computer Simulation of Powder Spectra*; ESR Symposium, 21st. Rocky Mountain Conference, Denver, CO, 1979.
(47) Beratan, D. N.; Hopfield, J. J. *J. Am. Chem. Soc.* **1984**, *106*, 6, 1584−1594.
(48) Beratan, D. N.; Onuchic, J. N.; Hopfield, J. J. *J. Chem. Phys.* **1987**, *86*, 4488−4498.
(49) Beratan, D. N.; Onuchic, J. N. *Photosynth. Res.* **1989**, *22*, 173−186.
(50) Beratan, D. N.; Onuchic, J. N.; Betts, J. N.; Bowler, B. E.; Gray, H. B. *J. Am. Chem. Soc.* **1990**, *112*, 7915−7921.
(51) Beratan, D. N.; Betts, J. N.; Onuchic, J. N. *Science* **1991**, *252*, 1285−1288.
(52) Beratan, D. N.; Betts, J. N.; Onuchic, J. N. *J. Phys. Chem.* **1992**, *96*, 2852−2855.
(53) Betts, J. N.; Beratan, D. N.; Onuchic, J. N. *J. Am. Chem. Soc.* **1992**, *114*, 4043−4046.
(54) Onuchic, J. N.; Beratan, D. N. *J. Chem. Phys.* **1990**, *92*, 722−733.
(55) Regan, J. J.; Onuchic, J. N. *Adv. Chem. Phys.* **1999**, *107*, 497−553.
(56) Curry, W. B.; Grabe, M. D.; Kunikov, I. V.; Skourtis, S. S.; Beratan, D. N.; Regan, J. J.; Aquino, A. J. A.; Beroza, P.; Onuchic, J. N. *J. Bioenerg. Biomembr.* **1995**, *27*, 285−293.

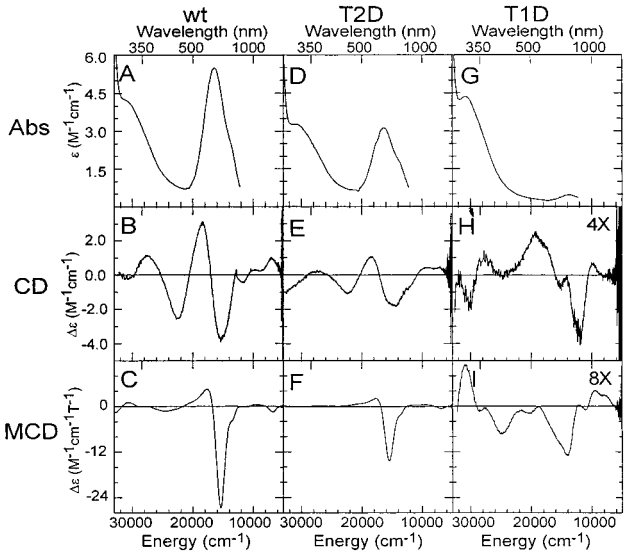

Figure 1. Optical spectra of Fet3p. (A) Absorption spectrum of wt at room temperature. (B) CD spectrum of wt at 4 °C. (C) MCD spectrum of wt at 5 K, 7 T. (D) Absorption spectrum of T2D at room temperature. (E) CD spectrum of T2D at 4 °C. (F) MCD spectrum of T2D at 5 K, 7 T. (G) Absorption spectrum of T1D at room temperature. (H) CD spectrum of T1D at 4 °C; *y*-axis is expanded by a factor of 4. (I) MCD spectrum of T1D at 5 K, 7 T; *y*-axis is expanded by a factor of 8.

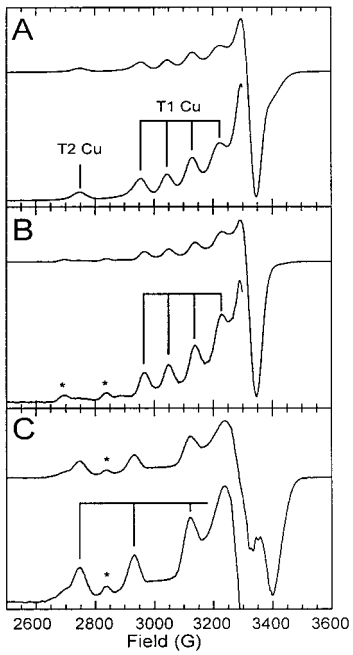

Figure 2. EPR spectra of Fet3p: (A) wt, (B) T2D, and (C) T1D. Conditions: microwave frequency, 9.515 GHz; temperature, 77 K; microwave power, 10 mW; modulation amplitude, 20 G; modulation frequency, 100 kHz; time constant, 0.5 s.

transitions of the T1, T2, and T3 Cu sites. These spectra are shown in Figure 1. The absorption spectrum of wt (Figure 1 A) is dominated by two envelopes of intense CT bands, one centered at 16 500 cm^{-1} with $\epsilon = 5500$ M^{-1} cm^{-1} (blue band), and one centered at 30 700 cm^{-1} with $\epsilon = 4300$ M^{-1} cm^{-1} (330 nm band), as reported previously.[32,33] The CD spectrum of wt at 4 °C (Figure 1 B) shows three intense bands at 15 300 (−), 18 400 (+), and 22 500 cm^{-1} (−), and four weak bands at 6900 (+), 9800 (+), 11 600 (−), and 27 500 cm^{-1} (+). The MCD spectrum of the wild-type protein at 5 K (Figure 1 C) is dominated by a very intense negative band at 15 400 cm^{-1}. Weaker bands are observed at 6800 (−), 9600 (+), 13 500 (−), 17 600 (+), 19 600 (+), 24 500 (−), 30 600 (+), and 32 900 cm^{-1} (−). The EPR spectrum of wt shows the typical T1 and T2 Cu signals (Figure 2 A), as previously reported. The RR spectrum of Fet3p obtained upon excitation at 647.1 nm is shown in Figure 3A. The most intense peak in the spectrum is at 434 cm^{-1}. Less intense peaks are observed at 417, 408, 401, and 393 cm^{-1}, and two weak peaks are observed at 459 and 485 cm^{-1}. This spectrum is typical for the RR spectra of blue Cu sites obtained upon excitation into the S π to Cu $d_{x^2-y^2}$ CT band, which typically consist of a number of vibrational transitions centered at ∼400 cm^{-1} that contain contributions from the Cu−S stretch.

The absorption spectrum of T2D is shown in Figure 1D. The blue band is ∼50% as intense as that in wild type, and the 330 nm band is ∼75% as intense. The T2D mutant is less stable, and the conditions (high protein concentration, 50% glycerol) and sample handling (deuteration by Centricon buffer exchange) required for CD and MCD inevitably resulted in loss of ∼50% of the blue band intensity. In addition, at least two new Cu signals were clearly evident in the EPR spectrum in the region of 2650−2920 G (indicated by the asterisks in Figure 2B). The T1 Cu EPR features are essentially the same as those in wild type, only about half as intense. Double integration of the T2D EPR spectrum yielded about half the total spin intensity as with the native protein, indicating that the extraneous Cu signals accounted for about half the total paramagnetic Cu in the sample.

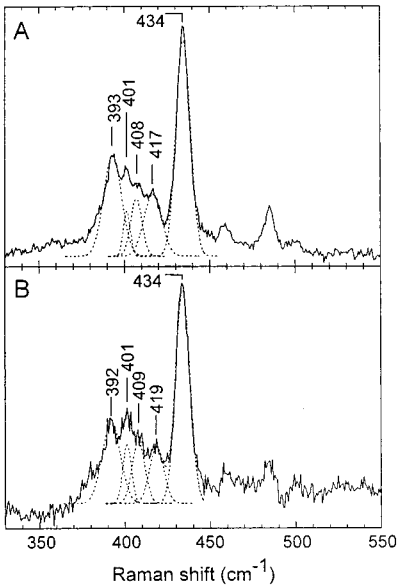

Figure 3. RR spectra of Fet3p upon excitation at 647.1 nm^{-1} (—) and spectral fit of the component vibrational peaks of predominantly Cu−SCys stretching character (- - -): (A) wt and (B) T2D.

The CD spectrum of T2D at 4 °C (Figure 1E) is dominated by the same three intense bands as in wild type, only at about half the intensity. The low-energy region, however, is distinctly different. Likewise, in the MCD spectrum of T2D at 5 K (Figure 1F), the bands at 6800, 13 500, 15 400, and 17 600 cm^{-1} are clearly evident but at about half the intensity as in wild type. A very broad, weak feature is observed at ∼9600 cm^{-1} (+). The three higher energy bands observed in the wt MCD spectrum are absent. The RR spectrum of T2D Fet3p obtained upon excitation at 647.1 nm is essentially identical to that of wt (Figure 3B).

The absorption spectrum of T1D (Figure 1G) is dominated by the intense 330 nm band arising from CT bands of the T3 Cu. A very weak envelope of bands is also evident at 13 800

cm^{-1}, with $\epsilon = 500\ M^{-1}\ cm^{-1}$. The EPR spectrum of T1D is shown in Figure 2C. It shows the T2 Cu signal, which is unchanged from that in wild type, and a small impurity Cu(II) signal at 2837 G (indicated by the asterisks in Figure 2C). Unlike in T2D, the Cu(II) impurity in T1D accounts for ≤10% of the total paramagnetic Cu. The CD spectrum of T1D at 4 °C (Figure 1H) shows the following bands: 9800 (+), 11 900 (−), 15 100 (−), and 19 300 cm^{-1} (+). The latter broad, intense band has a noticeable shoulder at ∼17 400 cm^{-1}. Two weak peaks are also seen at higher energy. The MCD spectrum of T1D at 5 K (Figure 1I) shows a large number of peaks. The most prominent bands are at 7900 (+), 9400 (+), 14 000 (−), 24 800 (−), and 30 800 cm^{-1} (+). The 14 000 cm^{-1} band has a prominent shoulder to higher energy. T1D Fet3p is not expected to yield peaks in the RR spectrum, since there are no intense CT bands at 647.1 nm, and this was indeed found to be the case (data not shown).

1.2. Analysis of the Spectroscopic Features of the Cu Sites. The optical spectra of wt Fet3p are dominated by the LF and CT transitions of the T1 Cu site. The optical spectra of the T1D mutant show that the T2 and T3 Cu transitions are much weaker but will still clearly contribute to the spectra of the wild-type protein. Therefore, to focus on the spectroscopic features of the T1 site, the contributions of the T2 and T3 Cu sites must be removed.

The T2D mutant suffers from reduced intensity of the T1 Cu spectral features and the presence of a large amount of extraneous paramagnetic Cu as shown by EPR. Nonetheless, the CD and MCD spectra are clearly dominated by the T1 Cu transitions, and the energies and relative intensities of these bands are essentially the same as those in the wild-type enzyme. The negative band at 24 800 cm^{-1} in the MCD spectrum of wt and T1D is clearly absent in the MCD spectrum of T2D, and therefore it can be ascribed to the T2 Cu site. The RR spectrum obtained upon excitation at 647.1 nm is only sensitive to vibrational bands of the T1 Cu site and will not be affected by contributions from extraneous Cu. Indeed, the RR spectrum of T2D FET3p is essentially identical to that of wild type. The similarity of the spectral features of the T1 Cu site in T2D to those of wild type shows that, although the T1 Cu site in this mutant is unstable, the electronic structure of the fraction that remains bound is not altered by the deletion of the T2 Cu site by mutagenesis.

The spectra reported in Figure 1G−I are of the cleanly isolated trinuclear Cu cluster of Fet3p. The only previous data on the electronic transitions of the trinuclear cluster of a multicopper oxidase are for T1HgLc.[19,20] The low-energy (5000−22 000 cm^{-1}) region of the CD and MCD spectra of T1HgLc consists of LF transitions of the T2 and T3 Cu sites, respectively. Five T3 Cu LF bands were resolved in the CD spectrum: 9200 (−), 11 100 (−), 13 900 (+), 15 300 (−), and 17 400 cm^{-1} (+). All four T2 Cu LF transitions were resolved in the MCD spectrum: 9400 (+), 12 100 (+), 14 100 (−), and 18 419 cm^{-1} (−). The CD and MCD spectra of T1D FET3 are qualitatively similar to those of T1HgLc. A few notable differences are observed, particularly in the MCD spectrum. A detailed comparison of trinuclear cluster of Fet3p with that of T1HgLc will be the subject of future study.

The spectroscopic features of the T1 Cu site of Fet3p could be readily isolated by subtracting the spectra of the T1D mutant from the wild-type spectra. The difference optical spectra are shown in Figure 4A−C. In the region of 5000−26 000 cm^{-1}, five bands were resolved in the CD spectrum and four bands were resolved in the MCD spectrum, with two shoulders clearly

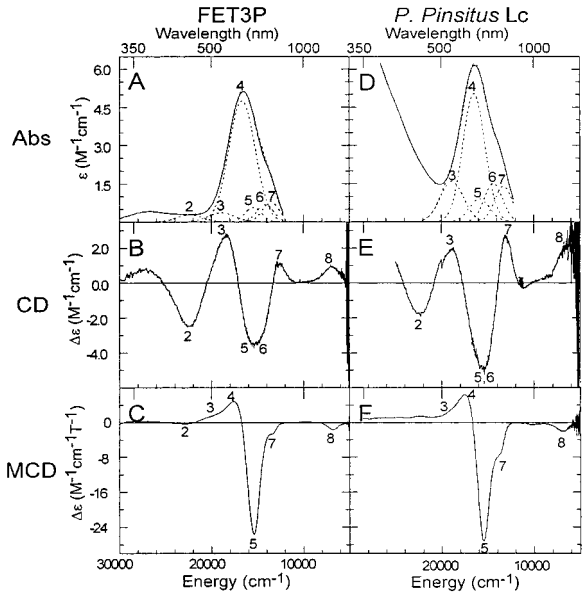

Figure 4. Optical spectra of the T1 Cu sites of Fet3p and *P. pinsitus* Lc. Bands are labeled as in ref 12 (see text). (A) Difference absorption spectrum of wt minus T1D Fet3p at room temperature (—) and resolved component Gaussian bands (- - -) from fitting of the absorption, CD, and MCD spectra. (B) Difference CD spectrum of wt minus T1D Fet3p at 4 °C. (C) Difference MCD spectrum of wt minus T1D Fet3p at 5 K, 7 T. (D) Absorption spectrum of resting oxidized *P. pinsitus* Lc at room temperature (—) and resolved component Gaussian bands (- - -) from fitting of the absorption, CD, and MCD spectra. (E) Difference CD spectrum of oxidized minus T1-reduced F-bound *P. pinsitus* Lc at 4 °C. (F) Difference MCD spectrum of oxidized minus T1-reduced F-bound *P. pinsitus* Lc at 5 K, 7 T. *P. pinsitus* Lc data are taken from ref 2.

evident. Iterative Gaussian fitting of the difference absorption, CD, and MCD spectra indicated that seven bands were required to fit the data. These are labeled on the spectra as bands 2−8, to be consistent with the numbering scheme of Pc.[12] The energies of these bands are listed in Table 1.

Previously, the spectroscopic features of the T1 Cu sites of several fungal Lc's were explored.[2] In fungal Lc, Cu-depleted mutants were not available, and instead, isolation of the spectroscopic features of the T1 Cu was accomplished by exploiting the dramatic negative shift in the redox potential of the trinuclear cluster upon F^- binding. Addition of ascorbate to F^--bound fungal Lc induces selective reduction of the T1 Cu site. Therefore, the features of the T1 Cu site could be obtained by subtraction of the F^--bound trinuclear cluster spectral features from the fully oxidized F^--bound spectra. The absorption spectrum of oxidized *Polyporous pinsitus*[57] Lc is shown in Figure 4D, and the CD and MCD spectra of the T1 Cu site of *P. pinsitus* Lc obtained as mentioned above are shown in Figure 4E,F. In the T1 Cu site of fungal Lc, the low-energy bands 5−8 were assigned as LF transitions. These originate from (in order of decreasing energy) the d_{xz}, d_{yz}, d_{xy}, and d_{z^2} orbitals (see Table 1 for the energies of these transitions in three different fungal Lc's). Band 6 is not resolved in the MCD spectrum but was needed in order to fit adequately the absorption and CD spectra. All of these LF transitions are 1500−2500 cm^{-1} higher in energy than the corresponding LF transitions in Pc, indicating an increase in the LF strength relative to four-coordinate blue Cu sites. In addition, the MCD sign of the $d_{z^2} \rightarrow d_{x^2-y^2}$ transition (band 8) is negative, rather than positive as seen in Pc. This was interpreted as being due to the lack of an axial ligand and a more trigonal planar geometry in the T1 Cu sites of the fungal

Table 1. Summary of the Optical, EPR, and RR Spectroscopic Data for the T1 Cu Site of Fet3p and Comparison to Those of Three Different Fungal Lc's

Electronic Transitions

		energy (cm^{-1})			
		Fet3p	*Polyporus pinsitus*[a]	*Myceliophthora thermophila*[a]	*Rhizoctonia solani*[a]
8	d_{z^2}	6 800	6 900	6 500	6 500
7	d_{xy}	13 500	13 300	13 200	13 100
6	d_{yz}	14 100	14 400	14 300	14 600
5	d_{xz}	15 400	15 900	15 500	15 900
4	S π	16 700	16 500	16 600	16 700
3	S pseudo-σ	18 900	18 900	18 700	18 600
2	N π	22 400	*b*	*b*	*b*

EPR Parameters

	Fet3p	*Polyporus pinsitus*[a]	*Myceliophthora thermophila*[a]	*Rhizoctonia solani*[a]
$g_{\|\|}$	2.202	2.194	2.201	2.208
$A_{\|\|}$ ($\times 10^{-4}$ cm^{-1})	88	90	87	82
$g_{\perp}$	2.046	2.046	2.045	2.043
$A_{\perp}$ ($\times 10^{-4}$ cm^{-1})	6	8	7	10
$\langle\nu_{Cu-S}\rangle$ from RR (cm^{-1})	417.8	413.0	419.7	435.7

[a] Taken from ref 2. [b] Not determined.

Lc's. Similarly, bands 3 and 4 were assigned as S pseudo-σ- and S π-to-Cu $d_{x^2-y^2}$ CT transitions, respectively.

The optical spectra of the T1 Cu site of Fet3p are remarkably similar to those of the fungal Lc's. Bands 3−8 of Fet3p occur at very similar energies and have the same signs and nearly the same intensities as those in fungal Lc; thus, they are readily assigned by comparison to the fungal Lc results (Table 1). In addition, band 2 is clearly evident in the absorption, CD, and MCD data. This band was assigned in Pc as a His N π-to-Cu $d_{x^2-y^2}$ CT transition,[12] and we assign it to the same transition in Fet3p. Thus, the T1 Cu site of Fet3p has the same unusually large LF strength as seen in the fungal Lc's and, therefore, a very similar trigonal planar geometry.

The EPR spectrum of the Fet3p T1 Cu site was also obtained by subtracting the spectra of the T1D mutant from the wild-type spectra (Figure S1 of the Supporting Information). The difference EPR spectrum was simulated with an axial spin Hamiltonian yielding $A_{||} = 88 \times 10^{-4}$ cm^{-1} and $g_{||} = 2.202$ (Table 1). These values are in the same range as those seen for the fungal Lc's:[2] $A_{||} = (82-90) \times 10^{-4}$ cm^{-1}, which is the highest of all blue Cu sites, and $g_{||} = 2.19-2.21$, which is among the lowest of all blue Cu sites. In the fungal Lc's, the low $g_{||}$ was ascribed to the increased LF strength (i.e., higher energy LF transitions), and the high $A_{||}$ was ascribed to the low $g_{||}$ and an increase in the amount of 4s mixing into the ground-state wave function, consistent with a more trigonal planar geometry. Since the T1 Cu site of Fet3 has the same comparatively large $A_{||}$, small $g_{||}$, and high LF strength from the optical data, this again indicates the geometric structure for this site is very similar to that of fungal Lc.

The resonance Raman (RR) spectra of blue Cu sites obtained upon excitation into the S π-to-Cu $d_{x^2-y^2}$ CT (Figure 3) consist of a number of vibrational transitions centered at ~400 cm^{-1} that are of predominantly Cu−S stretching character. The Cu−S stretching character is distributed over a number of different vibrational modes due to strong mechanical coupling encompassing the entire planar Cu−Cys side chain moiety.[58-60] The frequency of a metal−ligand stretching mode can be used to gauge the strength of the metal−ligand bond through the empirical correlation, Badger's rule. In the blue Cu sites, since the Cu−S stretching character is distributed over many modes, the intensity-weighted average of the Cu−S vibrational modes, $\langle\nu_{Cu-S}\rangle$, is used.[61]

In the RR spectrum of Fet3p obtained upon excitation at 647.1 nm (Figure 3), an intense peak is seen at 434 cm^{-1}, and less intense peaks are seen at 393−417 cm^{-1}. From a spectral fit of these bands, $\langle\nu_{Cu-S}\rangle = 417.8$ cm^{-1}. The RR spectrum of T2D Fet3p (Figure 3B) obtained upon excitation at 647.1 nm is essentially identical to that of the native protein, and the value of $\langle\nu_{Cu-S}\rangle$ is the same. It was found that in the T1 Cu sites of fungal Lc's, which lack an axial Met ligand, $\langle\nu_{Cu-S}\rangle$ is higher than in classical blue Cu sites that have an axial Met ligand, such as Pc. For example, $\langle\nu_{Cu-S}\rangle = 413$ cm^{-1} in *P. pinsitus* Lc, 421 cm^{-1} in *Polyporous versicolor* Lc, and 436 cm^{-1} in *Rhizoctonia solani* Lc (Table 1), while in Pc it is only 403 cm^{-1}.[2,61] The higher $\langle\nu_{Cu-S}\rangle$ found in the three-coordinate T1 Cu sites of fungal Lc's has been determined to correlate with an increase in the covalency of the $Cu-S_{Cys}$ bond, which is associated with an increase in the strength of this bond.[2] The value of 417.8 cm^{-1} for $\langle\nu_{Cu-S}\rangle$ for Fet3p is well within the range observed for the fungal Lc's, again indicating an increased $Cu-S_{Cys}$ covalency and bond strength.

To summarize, all of the above spectroscopic data support an electronic structure for the T1 Cu site of Fet3p that is nearly identical to that of fungal Lc, which in turn indicates that the T1 Cu site of Fet3p has the same three-coordinate planar geometry.

2. Reactivity. 2.1. Redox Potential. The reduction potential of the T1 Cu site of Fet3p was determined by the poised potential method with the $[Fe(CN)_6]^{3-}/[Fe(CN)_6]^{4-}$ redox couple. In pH 7.0 phosphate buffer, the potential is 427 ± 10 mV (Figure 5). In MES buffer, an accurate potential measurement could not be obtained because the equilibrium of the $[Fe(CN)_6]^{3-}/[Fe(CN)_6]^{4-}$ couple is perturbed by the buffer.[62]

(57) The fungi species *Polyporous versicolor* and *Polyporous pinsitus* have recently been renamed *Trametes versicolor* and *Trametes villosa*, respectively; herein we shall keep to the original names to be consistent with the previous literature.

(58) Urushiyama, A.; Tobari, J. *Bull. Chem. Soc. Jpn.* **1990**, *63*, 1563−1571.

(59) Dave, B. C.; Germanas, J. P.; Czernuszewicz, R. S. *J. Am. Chem. Soc.* **1993**, *115*, 12175−12176.

(60) Qiu, D.; Dong, S.; Ybe, J. A.; Hecht, M. H.; Spiro, T. G. *J. Am. Chem. Soc.* **1995**, *117*, 6443−6446.

(61) Blair, D. F.; Campbell, G. W.; Schoonover, J. R.; Chan, S. I.; Gray, H. B.; Malmstron, B. G.; Pecht, I.; Swanson, B. I.; Woodruff, W. H.; Cho, W. K.; English, A. M.; Fry, H. A.; Lum, V.; Norton, K. A. *J. Am. Chem. Soc.* **1985**, *107*, 5755−5766.

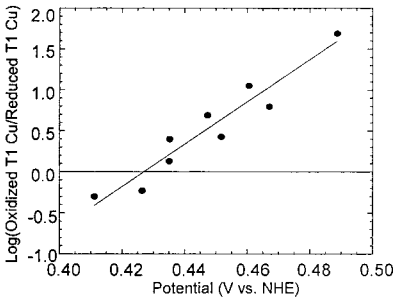

Figure 5. Poised potential titration of Fet3p. Starting concentration of $K_3[Fe(CN)_6]$ was ~5 mM. Solid line is best fit of two data sets to the Nerst equation.

Table 2. Comparison of the Reduction Potentials of Blue Cu Sites with and without Axial Met Ligands

protein	$E°$ (mV vs NHE)	ref
Blue Cu Sites with an Axial Met Ligand		
Achromobacter cycloclastes nitrite reductase	240	63
Pseudomonas aeruginosa azurin	310	40
zucchini ascorbate oxidase	344	85
spinach plastocyanin	370	86
Rhusvernicifera laccase	434[a]	43, 87
human ceruloplasmin (redox-active T1 sites)	448	11
Thiobacillus ferrooxidans rusticyanin	680	64
Polyporous pinsitus laccase F463M	680	65
Blue Cu Sites without an Axial Met Ligand		
Pseudomonas aeruginosa azurin M121L	412	40
Saccharomyces cerevisiae Fet3p	427	this study
Myceliophthora thermophila laccase	~465	88
Scytalidium therophilum laccase	~505	88
Coprinus cinereus laccase	550[b]	4
Rhizoctonia solani laccase	~655	88
Polyporus pinsitus laccase	770	88
Polyporus versicolor laccase	778	43, 89
Thiobacillus ferrooxidans rusticyanin M148L	798	74
human ceruloplasmin (T1PR)	≥1000	10

[a] It was found that the potential of the T1 Cu site in *R.vernicifera* Lc is affected by the presence of higher concentrations of $[Fe(CN)_6]^{3-}/[Fe(CN)_6]^{4-}$. At low concentrations, the potential decreases to 394 mV. Such an effect has not been probed in hCp or Fet3p, in which the potentials reported here are in the presence of a high concentration of $[Fe(CN)_6]^{3-}/[Fe(CN)_6]^{4-}$; therefore, we have listed the higher number for *R.vernicifera* Lc in the table. [b] The conditions of this redox potential determination were not reported.

Blue Cu sites exhibit a large range of redox potentials. For those with an axial Met ligand, $E°$ ranges from 240 mV for the T1 site of nitrite reductase (a perturbed "green" Cu site)[63] to 680 mV for rusticyanin[64] and the *P. pinsitus* Lc mutant in which an axial Met was introduced by mutagenesis[65] (Table 2). For blue Cu sites without an axial ligand, $E°$ ranges from 412 mV for azurin in which the axial Met was mutated to Leu[40] to ≥1.0 V for the T1PR site of hCp.[10] Although several mutagenesis studies have shown that the absence of the axial Met ligand increases the redox potential by ~100 mV, clearly other factors also contribute. At 427 mV, the T1 Cu site of Fet3p has the lowest potential of any wild-type three-coordinate blue Cu site yet determined. For comparison, the redox-active T1 Cu sites of hCp (which have axial Met ligands) have a potential of ~450 mV.[11]

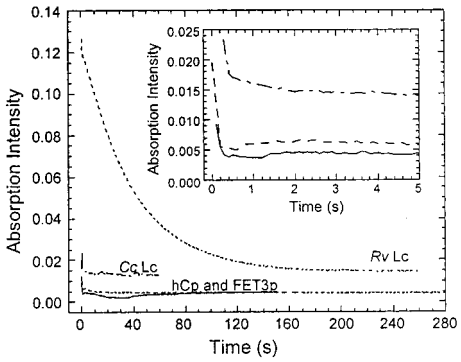

Figure 6. (A) Stopped-flow absorption data of reduction of the T1 Cu sites of hCp (—), Fet3p (— — —), *R. vernicifera* Lc (- - -), and *C. cinereus* Lc (— - —) with 7 equiv of Fe(II). Initial absorption at $t = 0$ was 0.32 for hCp and 0.13 for Fet3p, *R. vernicifera* Lc, and *C. cinereus* Lc. In the inset, the scale has been expanded to show the traces for hCp, Fet3p, and *C. cinereus* Lc.

2.2. Reduction Kinetics. Reduction of the T1 Cu site of several multicopper oxidases by Fe(II) was monitored by stopped-flow absorption spectroscopy. For Fet3p in MES buffer, even at the lowest concentration of Fe(II) used (7 equiv), reduction of the T1 Cu site was complete in <100 ms (Figure 6). For Cp, in which a very fast rate of reduction of the T1 Cu sites by Fe(II) has been previously reported,[66,67] the behavior was the same (Figure 6). This shows that for both Fet3p and hCp, the rate of reduction of the T1 Cu by a small excess of Fe(II) is very fast ($k_{obs} > 23\ s^{-1}$). Representative data of the reduction of the T1 Cu site of *R. vernicifera* Lc by Fe(II) (6 equiv) are shown in Figure 6. This kinetic trace could be fit to a single exponential, yielding $k_{obs} = 0.029\ s^{-1}$. The plot of k_{obs} versus Fe(II) concentration was linear up to a concentration of 12 equiv (Figure S2 of the Supporting Information), yielding a second-order rate constant of $1.79 \times 10^6\ M^{-1}\ s^{-1}$. This shows that Fe(II) is capable of reducing the T1 Cu site in *R. vernicifera* Lc, although far more slowly than in Fet3p and hCp. Reduction of the T1 Cu site of *C. cinereus* Lc by Fe(II) (6 equiv) was complete within 100 ms, yielding $k_{obs} > 23\ s^{-1}$; i.e., reduction of the T1 site in *C. cinereus* Lc by Fe(II) is >1000-fold faster than that in *R. vernicifera* Lc.

Reduction of the T1 Cu sites of *R. vernicifera* Lc, *C. cinereus* Lc, Fet3p, and hCp by the bulky organic substrate 1,4-hydroquinone was also examined by stopped-flow absorption spectroscopy at 25 °C. Representative data for the reduction of these enzymes by 1,4-hydroquinone (8 equiv) are shown in Figure 7 (inset). For Fet3p, the kinetics of reduction by 1,4-hydroquinone were studied in both phosphate and MES buffer, and no differences in the rate of reduction were observed. For *R. vernicifera* Lc and Cp, all of the kinetic experiments were performed in phosphate buffer. For each of these three enzymes, the kinetic traces were fit with a single-exponential expression to obtain k_{obs}, which is plotted versus equivalents of 1,4-hydroquinone in Figure 7. Two features are immediately apparent: (1) none of the enzymes exhibit any evidence of saturation behavior up to the maximum 1,4-hydroquinone concentration employed, and (2) the differences in rate of reduction of the three enzymes by 1,4-hydroquinone are large. The lack of saturation behavior indicates that in the range of

(62) A potentiometric titration of ferricyanide with ferrocyanide showed that this redox couple is unstable in MES buffer and does not follow the Nernst equation. This buffer effect is not observed in phosphate buffer (Figure S3 of Supporting Information).

(63) Suzuki, S.; Kohzuma, T.; Deligeer; Yamaguchi, K.; Nakamura, N.; Shidara, S.; Kobayashi, K.; Tagawa, S. *J. Am. Chem. Soc.* **1994**, *116*, 11145−11146.

(64) Ingledew, W. J.; Cobley, J. G. *Biochim. Biophys. Acta* **1980**, *590*, 141−158.

(65) Xu, F.; Palmer, A. E.; Yaver, D. S.; Berka, R. M.; Gambetta, G. A.; Brown, S. H.; Solomon, E. I. *J. Biol. Chem.* **1999**, *274*, 12372−12375.

(66) Osaki, S.; Walaas, O. *J. Biol. Chem.* **1967**, *242*, 2653−2657.

(67) Carrico, R. J.; Malmström, B. G.; Vänngård, T. *Eur. J. Biochem.* **1971**, *22*, 127−133.

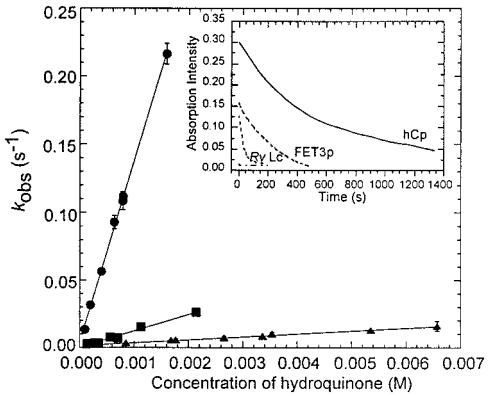

Figure 7. Plot of k_{obs} versus concentration of hydroquinone for *R. vernicifera* Lc (●), Fet3p (■), and Cp (▲).The least-squares best fits are shown (—). Inset: stopped-flow absorption data of reduction of the T1 Cu sites of hCp (—), Fet3p (— — —), *R. vernicifera* Lc (- - -), and *C. cinereus* Lc (— - —) with 8 equiv of hydroquinone. Initial absorption at $t = 0$ was 0.32 for hCp and 0.13 for Fet3p, *R. vernicifera* Lc, and *C. cinereus* Lc.

Table 3. Comparison of the Second-Order Rate Constants for Reduction of the T1 Cu Site by 1,4-Hydroquinone for Three Different Multicopper Oxidases

enzyme	rate (M^{-1} s^{-1})
R. vernicifera Lc	3.86×10^6
Fet3p	3.49×10^5
hCp	6.12×10^4 [a]

[a] Note that there are two redox-active T1 Cu sites in hCp; thus, the second-order rate constant per Cu site is half this value.

substrate concentrations used, substrate binding is nonexistent or very weak. The lack of substrate binding has been previously noted for *R. vernicifera* Lc from steady-state kinetic data.[68] The fact that hCp is a much less efficient enzyme toward organic substrates compared to *R. vernicifera* Lc has also been previously noted by steady-state kinetics.[69,70] The least-squares best fits to the plots of k_{obs} versus equivalents of 1,4-hydroquinone yield the following second-order rate constants for the reduction of T1 Cu: 3.86×10^6 M^{-1} s^{-1} for *R. vernicifera* Lc, 3.49×10^5 M^{-1} s^{-1} for Fet3p, and 6.12×10^4 M^{-1} s^{-1} for hCp (Table 3). Since hCp contains two redox-active T1 Cu sites, the second-order rate constant per T1 Cu site should be half this value, or 3.06×10^4 M^{-1} s^{-1}. These values are listed in Table 3. The second-order rate constant for *R. vernicifera* Lc is consistent with the previously reported results.[71−73] Reduction of *C. cinereus* Lc by 1,4-hydroquinone was also examined. Even at the lowest concentration of substrate (∼6 equiv), the reaction was complete in 100 ms, yielding $k_{obs} > 23$ s^{-1}. This indicates that reduction of the T1 Cu site of this enzyme by 1,4-hydroquinone is significantly faster than that in *R. vernicifera* Lc.

In summary, reduction of the T1 Cu site in *C. cinereus* Lc is extremely fast with both Fe(II) and 1,4-hydroquinone, while in *R. vernicifera* Lc it is moderately fast with 1,4-hydroquinone and slow with Fe(II), and in hCp and Fet3 it is slow with 1,4-hydroquinone but fast with Fe(II).

Discussion

We have examined the spectroscopy of the T1 Cu site of Fet3p in detail. From comparison of the optical, EPR, and RR spectra of the T1 Cu site of Fet3p with those of fungal Lc, it is readily apparent that the electronic structures of these sites are very similar. In particular, in Fet3p the LF transitions in the optical spectra are at higher energy than in the classical four-coordinate blue Cu sites such as Pc. In the EPR spectrum, the $g_{||}$ value is on the low end of blue Cu sites. In the fungal Lc's, this was ascribed to the increase in energy of the $d_{x^2-y^2} \rightarrow d_{xy}$ transition relative to that in Pc, and in Fet3p, this transition is at a comparably high energy. The $A_{||}$ value is at the upper end of all blue Cu sites, in part due to the low $g_{||}$, which derives from the higher energy of the $d_{x^2-y^2} \rightarrow d_{xy}$ transition. DFT calculations on the T1 Cu site of fungal Lc also showed a contribution from the increase in the amount of 4s mixing into the ground-state wave function due to the planar geometry. The $\langle \nu_{Cu-S} \rangle$ determined from the RR data is significantly higher than for four-coordinate blue Cu sites, consistent with a stronger and more covalent Cu $d_{x^2-y^2}$—Cys S π bond.[2] This remarkable similarity in the electronic structure of the T1 Cu site of Fet3p compared to that of fungal Lc indicates that this site has the same unusual three-coordinate planar geometry as that seen in *C. cinereus* Lc by X-ray crystallography.

The lack of an axial Met ligand in blue Cu sites has been demonstrated by mutagenesis in several systems to be responsible for an approximately 100 mV increase in the redox potential.[40,65,74] Among wild-type fungal Lc's, $E°$ for the T1 Cu site ranges from 465 to 778 mV versus NHE. Among wild-type classic four-coordinate blue Cu sites, $E°$ ranges from 310 to 680 mV. The perturbed "green" T1 site of nitrite reductase has an axial Met ligand but with a short Cu−S bond length, a very different electronic structure[14] and a much lower redox potential (240 mV).[63] The T1 Cu site in stellacyanin has a stronger Gln O ligand in place of the Met, and this leads to a still lower redox potential (180 mV).[75] The redox potential of the T1 Cu site of Fet3p in phosphate buffer is 427 mV, presently the lowest of any wild-type three-coordinate blue Cu site. For comparison, the redox potentials of the four coordinate T1 Cu sites in the well-characterized multicopper oxidases (*R. vernicifera* Lc, AO, and hCp) measured under the same conditions (in phosphate buffer) range from 344 to 448 mV (see Table 2). It is clear that while the axial Met ligand is responsible for a ∼100 mV difference in the blue Cu redox potential, the protein matrix (i.e., differences in orientation of backbone amide dipoles, hydrogen bonds, etc.) can tune the potential over a wide range.[76,77] Fet3p is at the low end of the three-coordinate $E°$ range, and *R. vernicifera* Lc and Cp are in the middle of the four-coordinate $E°$ range. Interestingly, Fet3p and Cp have very similar T1 Cu redox potentials despite their different electronic and geometric structures. This similar redox potential, however, is consistent with their similar ferroxidase function.

The kinetics of reduction of the T1 Cu sites by both Fe(II) and 1,4-hydroquinone show dramatic differences among the four enzymes studied. In the case of both hCp and Fet3p, reduction of the T1 Cu site by 6−7 equiv of Fe(II) is extremely fast ($k_{obs} > 23$ s^{-1}). Steady-state kinetic analysis has shown that

(68) Peterson, L. C.; Degn, H. *Biochim. Biophys. Acta* **1978**, *526*, 85−92.
(69) Peisach, J.; Levine, W. G. *J. Biol. Chem.* **1965**, *240*, 2284−2289.
(70) Young, S. N.; Curzon, G. *Biochem. J.* **1972**, *129*, 273−283.
(71) Holwerda, R. A.; Gray, H. B. *J. Am. Chem. Soc.* **1974**, *96*, 6008−6022.
(72) Andréasson, L.-E.; Reinhammar, B. *Biochim. Biophys. Acta* **1976**, *445*, 579−597.
(73) Andréasson, L.-E.; Reinhammar, B. *Biochim. Biophys. Acta* **1979**, *568*, 145−156.
(74) Hall, J. F.; Kanbi, L. D.; Strange, R. W.; Hasnain, S. S. *Biochemistry* **1999**, *38*, 12675−12680.
(75) Guckert, J. A.; Lowery, M. D.; Solomon, E. I. *J. Am. Chem. Soc.* **1995**, *117*, 2817−2844.
(76) Stephens, P. J.; Jollie, D. R.; Warshel, A. *Chem. Rev.* **1996**, *96*, 2491−2513.
(77) Warshel, A.; Papazyan, A.; Muegge, I. *J. Biol. Inorg. Chem.* **1997**, *2*, 143−152.

k_{cat} for enzyme turnover with Fe(II) as substrate is much lower than that in hCp (138 or 550 min^{-1}, depending upon the method of analysis),[25,26] and lower still in Fet3p (9.5 min^{-1}),[31,33] indicating that under steady-state conditions, reduction of the T1 Cu by Fe(II) is not the rate-limiting step in either enzyme. This step is likely to be the electron transfer from the T1 Cu site to the trinuclear cluster.[1] Reduction of the T1 Cu site of *C. Cinereus* Lc by 6−7 equiv of Fe(II) is also fast ($k_{obs} > 23\ s^{-1}$), while in *R. vernicifera* Lc, it is much slower ($k_{obs} = 0.029\ s^{-1}$). In the kinetics of reduction of the T1 Cu sites by 1,4-hydroquinone, for hCp, Fet3p, and *R. vernicifera* Lc, no evidence of saturation behavior was observed, and thus, this reaction is purely second-order. The second-order rate constant varies greatly among the three enzymes: reduction of the T1 Cu site of *R. vernicifera* Lc is ∼10-fold faster than that in Fet3p, which in turn is ∼10-fold faster than that in hCp. Reduction of the T1 Cu site of *C. Cinereus* Lc is by far the fastest: at the lowest concentration of 1,4-hydroquinone used, the lower limit of k_{obs} was 23 s^{-1}. This is >1000-fold faster than the rate of reduction of the T1 Cu site of *R. vernicifera* Lc with the same concentration of 1,4-hydroquinone.

The differences in the reactivities of these two substrates among the four enzymes can be interpreted in terms of semiclassical theory. The semiclassical equation for the rate of *inter*molecular ET, k_{ET}, is dependent upon the following: the electronic coupling matrix element (H_{AB}), the driving force ($\Delta G°$), the reorganization energy (λ), the steric term (S), and the equilibrium constant for formation of the interaction complex (K_A).[78]

$$k_{ET} = SK_A(4\pi^3/h^2\lambda kT)^{1/2}(H_{AB})^2 \exp[-(\Delta G° + \lambda)^2/4\lambda kT] \quad (1)$$

Since the substrate is the same for all three reactions, the observed differences in k_{ET} can be ascribed to the differences in the protein.

The difference in reduction rates for the T1 sites in *R. vernicifera* Lc and *C. cinereus* Lc can be ascribed to several factors. The redox potentials of the T1 Cu site of these two enzymes differ by ∼150 mV (Table 2, using the lower value of 394 mV for *R. vernicifera* Lc). This is predicted to increase the rate of reduction of *C. cinereus* Lc by up to 15-fold. Also, the greater covalency and the lack of an axial ligand in the case of the three-coordinate site of fungal Lc is expected to decrease the inner-sphere contribution to the reorganization energy by a modest amount, although this difference has not yet been experimentally determined. This will also tend to increase the rate. Simultaneously increasing the redox potential by 150 mV and decreasing the reorganization energy by 0.15 eV would increase the rate by up to 50-fold, significantly below the >1000-fold difference observed experimentally.

The other factors to consider are S, K_A, and H_{AB}. The S term accounts for the fact that only a limited set of orientations of the substrate and the active site of the protein will be appropriate for ET, while K_A is the equilibrium constant of formation of the interaction complex between the donor and the acceptor. The relative contribution of H_{AB} to k_{ET} can be analyzed with the Pathways program developed by Beratan and Onuchic.[47−56] In this model, H_{AB} is proportional to the product of decay factors associated with covalent bonds, ϵ_C, hydrogen bonds, ϵ_H, and space jumps, ϵ_S, along a given pathway:

$$H_{AB} \propto \prod\epsilon_C \prod\epsilon_H \prod\epsilon_S \quad (2)$$

The coupling decay across one covalent bond, ϵ_C, empirically is found to be 0.6. Decay across a space jump is exponential with distance, R. Hydrogen bonds are considered equal to covalent bonds; therefore, from heavy atom to heavy atom the coupling decay is ϵ_C^2. We have allowed for exponential decay of the ϵ_H term for longer hydrogen bonds. Thus,

$$\epsilon_C = 0.6$$
$$\epsilon_S = \epsilon_C \exp[-1.7(R - 1.4)]$$
$$\epsilon_H = \epsilon_C, \quad R \le 2.1\ Å$$
$$\epsilon_H = \epsilon_C \exp[-1.7(R - 2.8)], \quad R > 2.1\ Å \quad (3)$$

Coupling of the metal d-orbitals into and out of the pathway (i.e., covalency) must also be considered, but since all of the input pathways to the T1 Cu site examined herein involve the $Cu-N_{His}$ bond, this term will be similar for all. For *inter*molecular ET,[56] the coupling used is the maximum coupling between the T1 Cu site and all solvent-exposed atoms, as determined by use of a Connelly surface with a 2.0 Å probe radius.

After accounting for differences in $\Delta G°$ and λ, the remainder of the difference in rates for *R. vernicifera* Lc and *C. cinereus* Lc likely arises from differences in S, K_A, and H_{AB}. In the crystal structure of *C. cinereus* Lc, the imidazole ring of the T1 Cu-binding ligand His457 is directly solvent exposed and lies at the bottom of a relatively shallow and open bowl (see Figure 8A). Thus, there is little evidence from the crystal structure for a specific substrate binding site, and the T1 Cu site is highly accessible to large substrates. Thus, this solvent-exposed imidazole likely serves as the ET site for both Fe(II) and hydroquinone. Also, the ET pathway from the imidazole ring protons to the T1 Cu site will be three bonds, not including the metal−ligand bond, yielding a total coupling decay of 0.216, which indicates a very favorable ET pathway. Since there is no crystal structure available for *R. vernicifera* Lc, it is not possible to further assess the relative contributions of S, K_A, and H_{AB}. Nonetheless, it is clear that at least one of these terms is smaller in *R. vernicifera* Lc for both substrates.

In contrast to the two laccases, hCp and Fet3p exhibit large differences in the rate of reduction with the two substrates, while between these enzymes, the differences in rate for a given substrate are minor. The redox potentials of the T1 Cu sites are approximately the same and are between those of *R. vernicifera* Lc and *C. cinereus* Lc. The crystal structure of hCp shows that the T1 Cu sites are far more buried than in *C. cinereus* Lc (see Figure 8B). No ligands of the redox-active T1 Cu sites of Cp are solvent exposed; instead, the T1 Cu sites are buried ∼10 Å beneath the surface. In addition, they lie at the bottom of a long, narrow, highly negatively charged channel and directly beneath the divalent metal ion binding site.[8]

Interestingly, in hCp, two of the residues that are believed to be part of the site for Fe(II) binding are also the solvent-exposed residues with the largest electronic matrix coupling element (H_{AB}) with the T1 Cu. For the T1 Cu site in domain 6, which is coupled to the trinuclear cluster via the CysHis pathway ($T1_{CysHis}$), the solvent-exposed atom with the best coupling is the Glu272 Oϵ2. The Glu side chain is H-bonded to His1026 Hϵ2; this imidazole is one of the ligands at this type 1 Cu site (Figure 8B). Including this H bond, the coupling from the lone pair orbitals on Glu272 Oϵ2 to the T1 Cu site travels across seven bonds, yielding a coupling of 0.0280. The next best

(78) Marcus, R. A.; Sutin, N. *Biochim. Biophys. Acta* **1985**, *811*, 265−322.

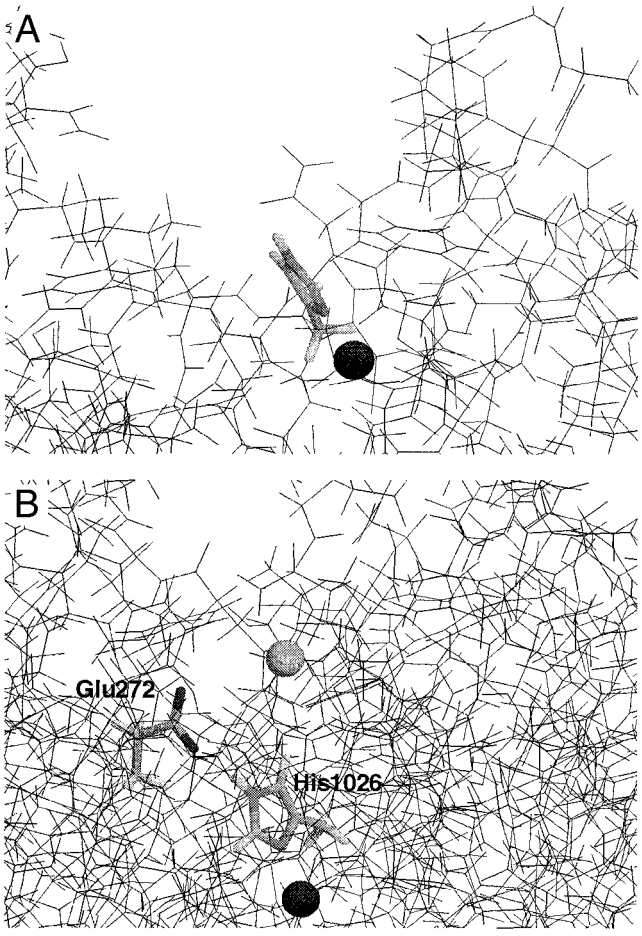

Figure 8. Illustration of the T1 Cu site accessibility in *C. cinereus* Lc (A) and hCp (B), taken from the X-ray crystal structures.[4,8] His457 is shown in *C. cinereus* Lc (A); Glu272 and His1026 are shown in hCp (B). Dark spheres represent Cu sites, and the lighter sphere represents the Fe(II) binding site in hCp, which is about ~10 Å from the T1 Cu site.

coupling from the surface is from an Asp residue (1025 Oδ2) with a coupling value of 0.00813. A similar picture exists for the other redox-active T1 Cu site in domain 4 ($T1_{Remote}$). Qualitatively then, in Cp, the product $SK_A(H_{AB})^2$ (eq 1) should be much larger for Fe(II) than for a comparatively bulky substrate such as 1,4-hydroquinone. Thus, the large difference in the rate of reduction of the T1 Cu in Cp by Fe(II) versus 1,4-hydroquinone most reasonably is a direct result of specific Fe(II)-binding.

No crystal structure is currently available for Fet3p. However, recent pulsed EPR data show the presence of bulk water in the second coordination sphere of the T1 Cu site,[79] indicating that it is quite close to the surface, unlike in Cp. Thus, the difference in the rate of reduction of the T1 Cu site of Fet3p by Fe(II) versus 1,4-hydroquinone arises from one of two possibilities: either (1) the structure of the surface of Fet3p is such that it is inaccessible to bulkier substrates, but accessible to water and Fe(II), and thus 1,4-hydroquinone interacts at a different site on the surface with a much smaller H_{AB} and a potentially different K_A, or (2) the T1 Cu site is accessible to all molecules, but the formation of the interaction complex with Fe(II) is more favored than that with 1,4-hydroquinone (i.e., larger K_A for iron). In either case, our data show that Fet3p exhibits a high degree of selectivity for Fe(II).

(79) Aznar, C. P.; Kosman, D. J.; Hassett, R.; Yuan, D.; McCracken, J. *J. Am. Chem. Soc.*, submitted.

The existence of a specific metal ion binding site in Fet3p has been the source of speculation for some time. It is clear from the sequences of hCp and Fet3p that the divalent metal ion binding motif conserved in domains 4 and 6 in Cp is absent in Fet3p. Nonetheless, Murphy et al. compared the crystal structure of hCp with the amino acid sequence of Fet3p and noted a number of putative Fe-binding residues in the latter protein, e.g., Glu329, Glu334, Glu227, Glu230, Asp336, and Asp228.[80] Of these residues, three are conserved between Fet3p and its homologue, Fio1p, in *Schizosaccharomyces pombe*: Glu227, Asp228, and Glu330.[81,82] Mutation of any of these three residues to Ala resulted in normal ferroxidase activity, indicating that these residues are unlikely to participate in Fe binding. Calabrese and co-workers modeled Fet3p with the crystal structure of AO, with which it shares a substantially greater degree of homology than hCp.[83] They proposed that Glu185, Tyr354, and Asp409 constitute the Fe(II)-binding site. This was experimentally tested by Musci and co-workers, who generated mutants with Glu185 replaced by Ala and with Tyr354 replaced by Phe.[84] The Y354F mutant exhibited modest decreases in both steady-state ferroxidase and aromatic amine oxidase activity, but the E185A mutant exhibited a significant decrease in the steady-state ferroxidase activity. This indicates that at least Glu185 likely plays a role in defining substrate specificity. The transient kinetics studies presented here support specific Fe(II) binding in Fet3p, but further work is clearly needed to evaluate the nature of exogenous metal binding in this system.

In comparing Fet3p to the more extensively studied multicopper oxidases, *R. vernicifera* Lc, fungal Lc, and hCp, a number of generalizations can be made. In many of the plant and fungal Lc's, the physiologically relevant substrate is not known, but at least some of the fungal Lc's are generally believed to be involved in lignin degradation.[1] Given this, maximum substrate accessibility and a very high redox potential are clearly desirable. Although the lack of the axial ligand is not the only contribution to the unusually high redox potential found in many fungal Lc's, it may be required to achieve sufficiently high reduction potentials. In terms of its sequence, Fet3p is most homologous to the fungal Lc's and maintains the unusual three-coordinate T1 Cu geometry of the fungal Lc's. Nonetheless, the protein matrix tunes its potential to the low end of the range. In hCp, Fe(II) apparently binds to the enzyme immediately adjacent to the redox-active T1 Cu sites, while other substrates have limited accessibility to the T1 Cu sites. This may be an adaptation to minimize unwanted oxidation reactions. It is likely that Fet3p has adapted a similar strategy as well, and this may also be the reason for its comparatively low redox potential.

(80) Murphy, M. E. P.; Lindley, P. F.; Adman, E. T. *Protein Sci.* **1997**, *6*, 761−770.
(81) Askwith, C.; Kaplan, J. *J. Biol. Chem.* **1997**, *272*, 401−405.
(82) Askwith, C. C.; Kaplan, J. *J. Biol. Chem.* **1998**, *273*, 22415−22419.
(83) Bonaccorsi di Patti, M. C.; Pascarella, S.; Catalucci, D.; Calabrese, L. *Protein Eng.* **1999**, *12*, 895−897.
(84) Bonaccorsi di Patti, M. C.; Felice, M. R.; Camuti, A. P.; Lania, A.; Musci, G. *FEBS Lett.* **2000**, *472*, 283−286.
(85) Mondovi, B., Avigliano, L., Eds. A*scorbate Oxidase*; CRC Press: Boca Raton, FL, 1984; Vol. 3, pp 101−118.
(86) Katoh, S.; Shiratori, I.; Takamiya, A. *J. Biochem. (Tokyo)* **1962**, *51*, 32−40.
(87) Reinhammar, B. R. M.; Vänngård, T. I. *Eur. J. Biochem.* **1971**, *18*, 463−468.
(88) Xu, F.; Shin, W.; Brown, S. H.; Wahleithner, J.; Sundaram, U. M.; Solomon, E. I. *Biochim. Biophys. Acta* **1996**, *1292*, 303−311.
(89) Malmström, B. G.; Reinhammar, B.; Vänngård, T. *Biochim. Biophys. Acta* **1968**, *156*, 67−76.

An interesting and unexplored question in the chemistry of Fet3p is the trafficking of the product, Fe(III). In hCp, the T1 Cu sites are buried at the bottom of a long, narrow, and negatively charged crevice, beneath the divalent metal ion binding site. Situated above this, there is a large and more loosely ordered negatively charged patch that is believed to be the trivalent metal ion binding site.[8] These Fe(III) holding sites may function in short-range Fe(III) transport, shuttling up to four Fe(III) atoms between the putative membrane-bound Fe(II) donor and the ultimate Fe(III) acceptor in plasma, transferrin.[11] In Fet3p, the situation is quite different: it forms a specific enzyme complex with the Fe(III) acceptor, the iron permease Ftr1p. This is likely to affect the details of its ferroxidase mechanism. Thus, although the function of Fet3p may resemble that of hCp, in many ways it resembles a fungal Lc that has been adapted to perform ferroxidase chemistry.

Acknowledgment. We thank Dr. A. M. Brzozowski for providing *Coprinus cinereus* laccase, the Stanford Blood Center for providing human plasma, Dr. Sang-Kyu Lee for helpful discussions regarding kinetics, and Prof. Tom Wandless and Joe Barco for access to Insight II. This research was supported by NIH Grants DK31450 (to E.I.S.) and DK53820 (to D.J.K.).

Supporting Information Available: EPR spectrum of wt minus T1D Fet3p and simulated EPR spectrum of the T1 Cu site of Fet3p; reduction kinetics of the T1 Cu site of *R. vernicifera* Lc by Fe(II); and potentiometric titrations of ferricyanide with ferrocyanide in pH 6.5 phosphate and pH 6.5 MES buffers (PDF). This material is available free of charge via the Internet at http://pubs.acs.org.

JA003975S